Identification of vacancy complexes in Si by positron annihilation

2003 J. Phys.: Condens. Matter 15 S2791

(http://iopscience.iop.org/0953-8984/15/39/003)

INSTITUTE OF PHYSICS PUBLISHING JOURNAL OF PHYSICS: CONDENSED MATTER

J. Phys.: Condens. Matter **15** (2003) S2791–S2801 PII: S0953-8984(03)67266-8

Identification of vacancy complexes in Si by positron annihilation

K Saarinen and V Ranki

Laboratory of Physics, Helsinki University of Technology, PO Box 1100, 02015 HUT, Finland

Received 7 August 2003
Published 19 September 2003
Online at stacks.iop.org/JPhysCM/15/S2791

Abstract

We show that the detailed atomic structure of vacancy complexes in Si can be experimentally determined by combining positron lifetime and electron momentum distribution measurements. The divacancies, vacancy–oxygen complexes (A-centres) and vacancies paired with a donor impurity, V–P and V–As (E-centres), are identified in electron-irradiated Si. The formation of native vacancy defects is observed in highly As-doped Si at the doping level of 10^{20} cm^{-3}. The defects are identified as monovacancies surrounded by three As atoms. We verify the formation mechanism of these defects by annealing experiments in irradiated Si. We show that the migration of V–As pairs at 450 K leads to the formation of V–As_2 complexes, which convert to V–As_3 defects at 700 K. These results explain the electrical deactivation and clustering of As in epitaxial or ion-implanted Si during postgrowth heat treatment at 700 K.

1. Introduction

Vacancy defects in Si are elementary examples of deep centres in semiconductors. Their basic properties, such as electronic structure, lattice relaxations, migration temperatures and defect complex formation, have been very successfully studied by electron paramagnetic resonance (EPR) techniques since the 1950s [1]. According to these works, both the monovacancy and interstitial atom are mobile at low temperatures below 150 K. The vacancy defects surviving at room temperature are thus complexes formed by the migration of the elementary vacancy, such as divacancies (V_2), vacancy–oxygen (V–O) pairs (A-centres) and vacancy–donor impurity pairs (E-centres).

The formation of vacancy–impurity complexes has become an important issue in the miniaturization of Si field-effect transistors [2]. The decrease in the size of the transistor requires an increase in the doping density, both at the source and drain regions as well as in the channel. In the As and Sb doping of Si, however, the concentration of free electrons saturates at the level of $\leqslant 5 \times 10^{20}$ cm^{-3} when the impurity concentration is increased [3, 4]. This behaviour is indicative of the formation of inactive impurity clusters or compensating defects that trap free electrons. There is presently no consensus on the detailed nature of these

defects. Experimental evidence has been obtained on impurity precipitation as well as on the formation of vacancy–impurity complexes (see [5–10] and citations therein) and pairing of dopant atoms [7, 11]. Theoretical results propose that the vacancy–impurity complexes are formed very abundantly and they may also play distinct roles in the diffusion and clustering of impurities [6]. However, the number of vacancies and impurities in these complexes has remained unresolved in the experiments, partly since EPR experiments are generally difficult in thin overlayers and highly doped material. There is thus a need for new experimental information on the atomic structure of defects in heavily n-type Si.

Positron annihilation spectroscopy is a method for the direct identification of vacancy defects [12, 13]. Thermalized positrons in solids get trapped at neutral and negative vacancies because of the missing positive charge of the ion cores. At vacancies positron lifetime increases and positron–electron momentum distribution narrows due to the reduced electron density. The core electron momentum distribution can be used to identify the atoms surrounding the vacancy [14]. The experiments can be done both in resistive and highly conductive samples and also in thin layers by implanting positrons from a low-energy beam.

In this work we show that the combination of positron lifetime and core electron momentum distribution experiments yields quantitative and detailed information on the structure of vacancy complexes in Si. We present new data which demonstrate the power of positron annihilation experiments and their theoretical analysis in identifying the divacancies and V–O pairs in electron-irradiated Si. We also review our recent works [15–17] in highly n-type Si. The results indicate that the dominant vacancy defect in heavily As-doped Si is a vacancy surrounded by three As atoms (V–As_3). The formation of this defect takes place by subsequent migration of V, V–As and V–As_2, and it can be removed by high-temperature annealing followed by rapid cooling. The electrical deactivation and diffusion properties of As in Si will be discussed and the recent theoretical models will be commented on in the light of our experimental observations.

2. Experimental details and theoretical analysis

The divacancies and V–O pairs were studied in undoped float-zone (FZ) refined Si(100) and in lightly B-doped ($\rho = 8$–$15\ \Omega$ cm) Czochralski (Cz) grown Si(100) bulk crystals. Defects in highly n-type Si were investigated in Cz grown Si(111) bulk crystals doped with [As] $= 10^{19}$ and 10^{20} cm^{-3} and [P] $= 10^{20}$ cm^{-3}. Experiments were done both in as-grown samples as well as after 2 MeV electron irradiation at 300 K.

The positron experiments were performed in the conventional way by sandwiching two identical sample pieces with a 30 μCi ^{22}Na positron source [12, 13]. A fast–fast coincidence system with a time resolution of 230 ps was used in the positron lifetime experiments. The positron–electron momentum distribution was measured as a Doppler broadening of the 511 keV annihilation radiation, using a Ge detector with an energy resolution of 1.4 keV. In order to observe positron annihilations with core electrons, the experimental background was reduced by detecting simultaneously the two annihilation photons [14]. For this purpose, a second detector was placed collinearly with the Ge detector and a coincidence between the two detectors was electronically required.

In order to put the experimental identifications on a firmer basis we compared them with the calculated momentum distributions of annihilating electron–positron pairs [18–20]. In these works, the valence electron densities were calculated self-consistently employing the plane-wave pseudopotential method. Atomic wavefunctions were used for core electrons. A supercell of 64 atomic sites in a periodic superlattice was used to describe defects which were assumed to be ideal, i.e. the atoms were at the ideal lattice sites. Only the neutral

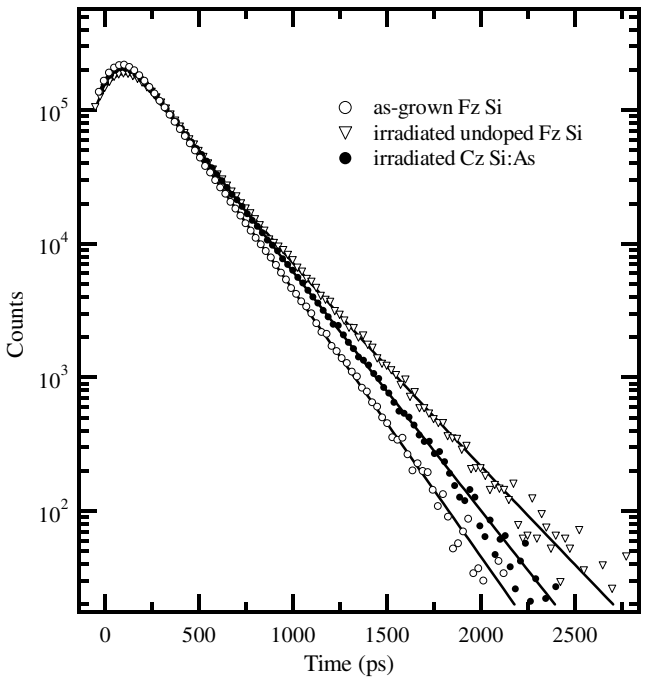

Figure 1. Positron lifetime spectra in as-grown and in 2 MeV electron-irradiated Si samples. Positrons annihilate in the as-grown sample with a single lifetime of 220 ps corresponding to delocalized positrons in the lattice. In the irradiated samples the experiments reveal vacancies with positron lifetimes of 250 ps (V–As pair in Cz Si:As sample doped with [As] $= 10^{20}$ cm^{-3}) and 300 ps (divacancy in undoped FZ Si sample).

defect states were considered in the calculations. The ensuing positron states and annihilation characteristics were calculated within the local density approximation for electron–positron correlation (parametrizations by Boronski and Nieminen [21] were used). The state-dependent enhancement scheme [18] was used in calculating the momentum distributions.

3. Vacancy defects in undoped and lightly p-type Si

The unirradiated FZ and Cz Si samples have only a single positron lifetime component of about 220 ps (figure 1), which is practically constant as a function of temperature [22]. This behaviour shows that no vacancies are observed by positrons and all annihilations take place at the delocalized state in the bulk lattice, with the lifetime $\tau_B = 220$ ps.

The presence of vacancy defects in electron-irradiated FZ Si samples is evident in figure 1. The lifetime spectrum has two components, the longer of which, $\tau_2 = 300 \pm 5$ ps, corresponds to positrons trapped at vacancy defects. The shorter lifetime component is $\tau_1 = 140$–180 ps. It is less than τ_B since it reflect both annihilation and trapping of delocalized positrons in the Si lattice. The lifetime of $\tau_2 = 300 \pm 5$ ps is clearly larger than expected for a monovacancy but it is equal to the calculated lifetime for annihilation at divacancies [19]. The positron results show that the charge state of divacancies is negative and their introduction rate is about $[V_2]/\Phi = 0.01$ cm^{-1} (Φ is the irradiation fluence) in 2 MeV electron irradiation [22]. These results are in good agreement with those obtained previously by EPR [1].

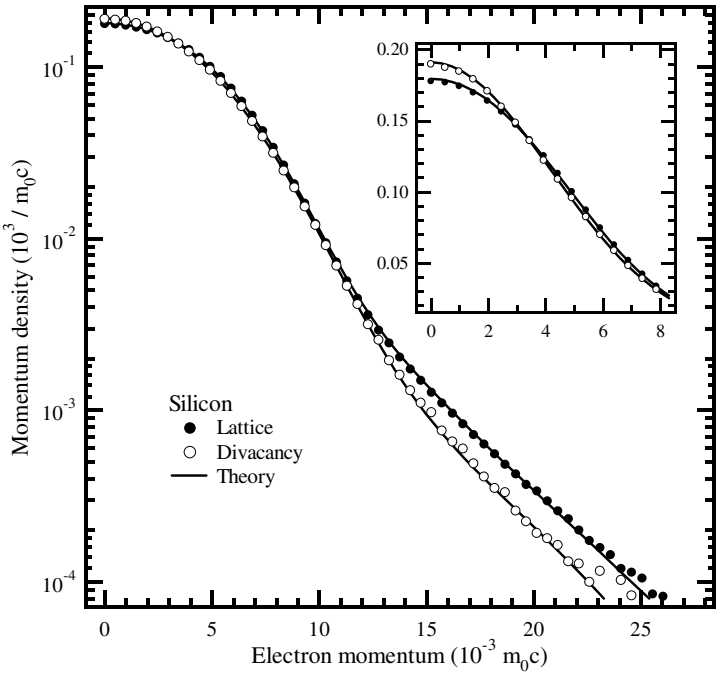

Figure 2. Positron electron momentum distributions measured for annihilations in the Si(100) lattice and at divacancies. The solid curve shows the theoretical results [19]. The experimental curve for the divacancy has been obtained by decomposing Doppler broadening data in 2 MeV electron-irradiated FZ and Cz Si samples with the help of positron lifetime experiments [22].

The positron lifetime spectra measured in electron-irradiated Cz Si samples show the presence of divacancies ($\tau = 300$ ps), but at low temperatures another positron trap with a much lower lifetime ($\tau = 230$ ps) is also observed [22]. This positron lifetime can be attributed to annihilations at V–O complexes [22]. The lifetime $\tau = 230$ ps is only slighly above that in a defect-free lattice ($\tau_B = 220$ ps), demonstrating that the open volume trapping positrons is less than that of a monovacancy. The positron results are in good agreement with the conventional model of the A-centre [1], which is formed from a vacant lattice site next to an oxygen atom. The O atom occupies a bond centre site between two adjacent Si atoms neighbouring the vacancy, which thus has a higher electron density and smaller open volume than an isolated monovacancy.

The Doppler broadening spectrum measured in Cz Si at 20 K is a superposition of the momentum distributions in the Si lattice $\rho_B(p)$, divacancies $\rho_{V2}(p)$ and V–O defects $\rho_{VO}(p)$. The positron lifetime spectra in Cz Si can be analysed with the kinetic trapping model, which yields the positron trapping rates and the fractions of annihilations at both V_2 and V–O defects [22]. This information can be used to decompose the Doppler broadening data. We measure $\rho_B(p)$ in the unirradiated reference sample and decompose $\rho_{V2}(p)$ and $\rho_{VO}(p)$ from a pair of Doppler spectra measured in two samples irradiated with different fluences.

The measured momentum density $\rho_{V2}(p)$ (figure 2) at the divacancy has the characteristic features of positron annihilation at vacancy defects. The valence electron density is lower at divacancies than in the perfect Si lattice, which is observed as a narrowing of the Doppler

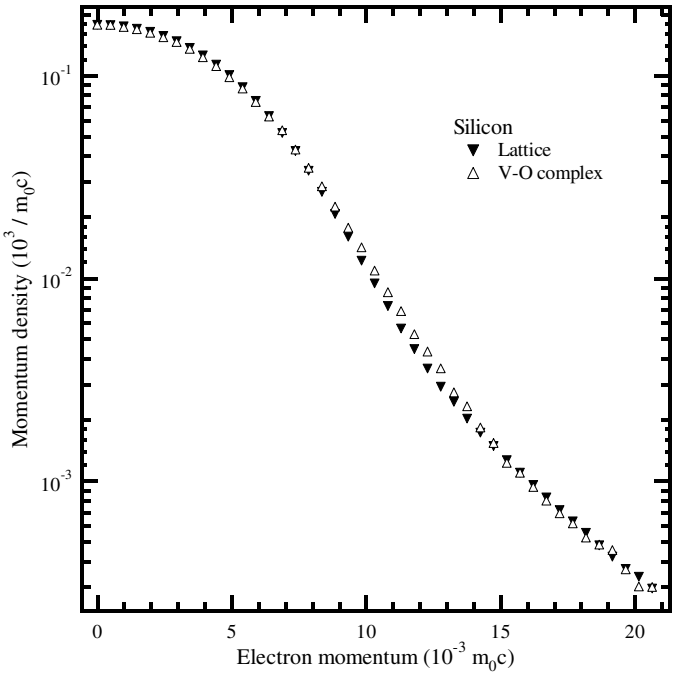

Figure 3. Positron electron momentum distributions measured for annihilations in the Si(100) lattice and at V–O complexes (A-centres). The result has been obtained by decomposing Doppler broadening data in 2 MeV electron-irradiated Cz Si samples by utilizing the positron lifetime experiments [22].

broadening spectrum of figure 2. The sensitivity of a Doppler experiment to vacancies is largest at low momenta of (0–2) $\times$ $10^{-3}m_0c$ and at high momenta of (10–25) $\times$ $10^{-3}m_0c$. The conventional S and W parameters are defined as integrals over these momentum regions, which correspond to those of valence electrons and outermost core electrons, respectively. The theoretical calculation [19] of the momentum density $\rho_{V2}(p)$ is in excellent agreement with the experimental results.

The measured momentum density $\rho_{VO}(p)$ at the V–O complex is broader than that obtained for the divacancy V_2 for the whole momentum region (0–20) $\times$ $10^{-3}m_0c$ shown in figures 2 and 3. This is expected, since the open volume and the valence electron density in V–O are much closer to those of the Si lattice than in the case of V_2, and the same effect is already observed in the positron lifetimes (220 for Si lattice, 230 ps for V–O and 300 ps for V_2). Interestingly, the valence electron region of $\rho_{VO}(p)$ at (0–10) $\times$ $10^{-3}m_0c$ is clearly broader than the momentum distribution in the Si lattice. This is due to the valence electrons of oxygen, which are more tightly bound to the O nucleus and have a much larger average momentum than those of Si. Positron annihilation experiments are thus able to identify the small open volume of the V–O complex by the low lifetime (230 ps) as well as the presence of O next to the vacancy by the broadening of the momentum distribution (figure 3).

To emphasize the characteristic features of positron annihilation at V_2 and V–O we have plotted the difference curves $\rho_{V2}(p) - \rho_B(p)$ and $\rho_{VO}(p) - \rho_B(p)$ in figure 4. The narrowing of the momentum distribution and the perfect agreement with theoretical calculations [19] is evident in the curve measured at a divacancy. The smaller general changes and the broadening effect due to the valence electrons of O are clearly seen for the V–O complex.

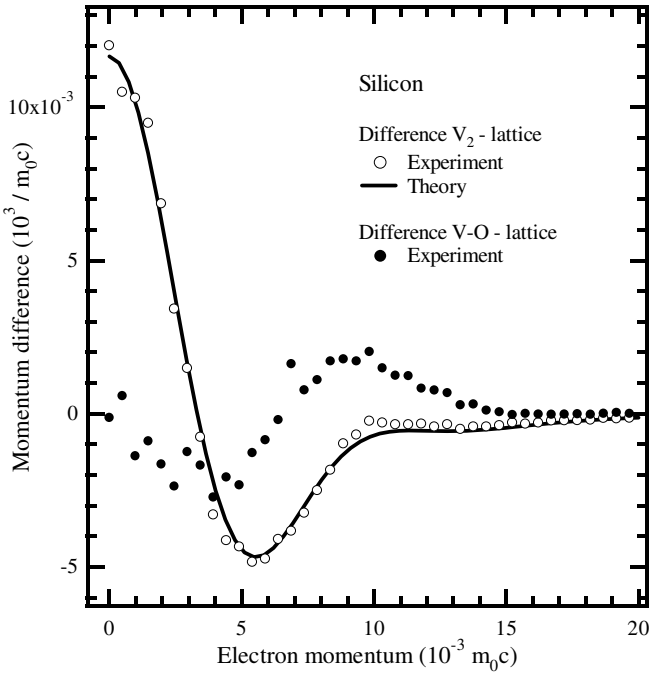

Figure 4. The difference curves of momentum distributions measured at divacancies and at V–O complexes. The result has been obtained by decomposing Doppler broadening data in 2 MeV electron-irradiated FZ and Cz Si samples and the difference was calculated by subtracting the momentum distribution in the bulk lattice. The solid curve shows the theoretical result for the divacancy [19].

4. Vacancy–impurity complexes in highly n-type Si

4.1. Positron lifetime results

The positron lifetime spectra in the as-grown Si([As] $= 10^{19}$ cm^{-3}) and Si([P] $= 10^{20}$ cm^{-3}) samples have a single component of about 220 ps at 300 K. The lifetime is the same as often reported for defect-free Si ($\tau_B = 220$ ps) [23], and depends very little on temperature. This behaviour is typical when all positrons annihilate at a delocalized state in the lattice, and can be attributed to the thermal expansion [12]. The Si([As] $= 10^{19}$ cm^{-3}) and Si([P] $= 10^{20}$ cm^{-3}) samples are thus free of vacancies trapping positrons.

The positron average lifetime is clearly higher in the as-grown Si([As] $= 10^{20}$ cm^{-3}) sample: $\tau_{av} = 232$ ps at 300 K. Furhermore, the lifetime spectrum has two components, the longer of which is $\tau_2 = 250 \pm 3$ ps. Both τ_{av} and τ_2 are almost constant as a function of temperature. The two-component lifetime spectrum and the increase of τ_{av} above the bulk lifetime τ_B are clear signs that native vacancies exist in the Si([As] $= 10^{20}$ cm^{-3}) sample. The second lifetime component $\tau_2 = 250 \pm 3$ ps is characteristic of the positron annihilations at a vacancy [12].

In all electron-irradiated samples the average positron lifetime is longer than in as-grown samples, indicating that irradiation-induced vacancies are observed (figure 1). In the Si(P : 10^{20}) sample irradiated to the fluence $\Phi = 5 \times 10^{17}$ cm^{-2} the lifetime spectrum can be decomposed and the vacancy component $\tau_2 = 250 \pm 3$ ps is thus obtained. Irradiated Si([As] $= 10^{20}$ cm^{-3}) samples have only a single positron lifetime of about 247 ± 2 ps, almost

independently of the irradiation fluence. This behaviour can be explained by a saturation of positron trapping at irradiation-induced vacancy defects. When the vacancy concentration exceeds 10^{18} cm^{-3} [12, 23], all positrons annihilate at the irradiation-induced vacancy defects with the lifetime 247 ± 2 ps and no annihilations take place at the delocalized bulk states or at the native vacancies detected before irradiation. The vacancy concentration of $\sim 10^{18}$ cm^{-3} is consistent with the expected introduction rate in electron-irradiated heavily n-type Si [1, 23, 24].

The same positron lifetime at the vacancy, $\tau_V = 248 \pm 3$ ps, is thus observed for three different types of samples: (i) as-grown Si([As] $= 10^{20}$ cm^{-3}), (ii) electron-irradiated Si([As] $= 10^{20}$ cm^{-3}), and (iii) electron-irradiated Si([P] $= 10^{20}$ cm^{-3}). The positron lifetime at the vacancy characterizes the open volume of the defect. According to experiments [23, 24] and theoretical calculations [19], the lifetime of 248 ± 3 is typical of the single vacancy in Si, whereas for a divacancy much larger values of about 300 ps are observed [19, 25, 26].

4.2. Identification of vacancy–impurity complexes by Doppler broadening measurement

In order to identify the monovacancies in detail, we have performed Doppler broadening experiments using the two-detector coincidence technique [14]. These measurements yield the one-dimensional momentum distribution of electrons as seen by the positron. In the samples containing vacancy defects we obtain the superimposed distribution $\rho(p) = (1 - \eta)\rho_B(p) + \eta\rho_V(p)$, where $\rho_B(p)$ and $\rho_V(p)$ are the momentum distributions in the lattice and at the vacancy, respectively. The lifetime results (figure 1) can be used to determine the fraction of positrons annihilating at vacancies $\eta = (\tau_{av} - \tau_B)/(\tau_V - \tau_B)$ [12]. Since the momentum distribution in the lattice $\rho_B(p)$ can be measured in the reference sample, the distributions $\rho_V(p)$ at vacancies can be decomposed from the measured spectrum $\rho(p)$. They are shown in figure 5 for the monovacancies observed in as-grown Si([As] $= 10^{20}$ cm^{-3}) as well as in irradiated Si([As] $= 10^{20}$ cm^{-3}) and Si([P] $= 10^{20}$ cm^{-3}).

The momentum distributions $\rho_V(p)$ at vacancies indicate large differences in the higher momenta ($p > 12 \times 10^{-3} m_0 c$), where the annihilation with core electrons is the most important contribution (figure 5). Since the core electron momentum distribution is a specific characteristic of a given atom, the differences between the spectra in figure 5 indicate different atomic environments of the vacancy in each of the three cases. Because both in Si ($Z = 14$) and P ($Z = 15$) the 2p electrons constitute the outermost core electron shell, the core electron momentum distributions of these elements are very similar. The crucial difference in the core electron structures of Si, P and As is the presence of 3d electrons in As. The overlap of positrons with the As 3d electrons is much stronger than with the more localized Si or P 2p electrons. The large intensity of the core electron momentum distribution is thus a clear sign of As atoms surrounding the vacancy.

The 2 MeV electron irradiation creates vacancies and interstitials as primary defects, both of which are mobile at 300 K [1]. In heavily n-type Si the donor atom may capture the vacancy and form a vacancy–impurity pair [1]. The monovacancy detected in heavily P-doped Si is thus the V–P pair. Similarly, it is natural to associate the electron irradiation-induced vacancy in Si([As] $= 10^{20}$ cm^{-3}) with a V–As pair. The influence of As next to the vacancy is clearly visible as the enhanced intensity in the high-momentum region (figure 5). An even stronger signal from As is seen in the as-grown Si([As] $= 10^{20}$ cm^{-3}). A linear extrapolation of the intensity of the distribution shows that the native complex is V–As$_3$, i.e. the vacancy is surrounded by *three* As atoms.

The identifications are confirmed by theoretical results [15, 19], which are in a very good agreement at both low and high momenta (figure 5). The theory reproduces the linear increase

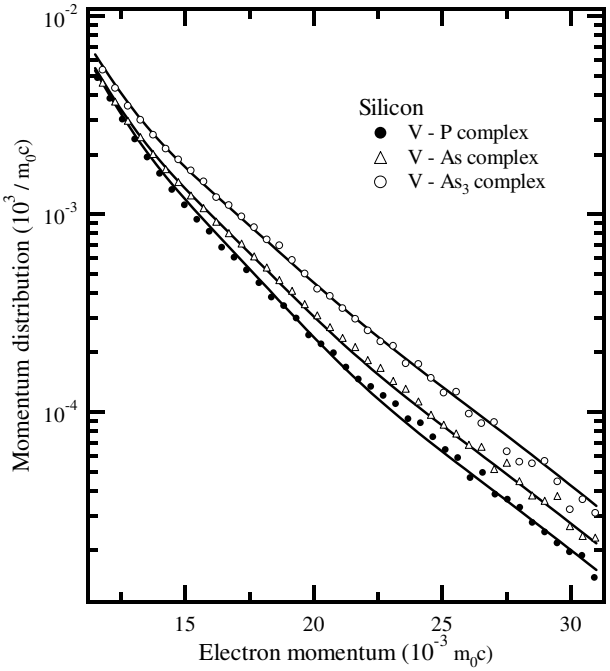

Figure 5. The high-momentum part of the positron–electron momentum distribution at the various vacancy–impurity pairs, identified in electron-irradiated Si([P] = 10^{20} cm^{-3}) (●) and in as-grown (○) and irradiated (△) Si([As] = 10^{20} cm^{-3}). The results of theoretical calculations are shown by the solid curves [15].

of the intensity of the core electron momentum distribution with increasing number of As atoms surrounding the vacancy. For the V–As_3 complex the agreement with the experimental result is excellent (figure 5), whereas the intensities calculated for V–As_2 and V–As_4 are much too small or large, respectively. In the valence electron momentum range, the calculated curves for V–As and V–As_3 also fit very well with the experiment. To conclude, the theoretical calculations strongly support the experimental defect identifications that (i) vacancies complexed with single donor impurities are detected in electron-irradiated P and As-doped Si, and (ii) the native defect in Si([As] = 10^{20} cm^{-3}) is a vacancy surrounded by three As atoms.

4.3. Formation of vacancy–impurity complexes by migration

The existence of V–As_3 complexes in heavily As-doped Cz Si is consistent with the defect formation and diffusion mechanisms described theoretically [6, 27–29]. The calculated formation energies of V–As_n ($n > 2$) complexes are negative, suggesting that total deactivation of As takes place at any doping level [5, 6]. The n-type conductivity of Si(As) is possible only because the creation of defect complexes is limited by kinetic processes such as the migration of defects [6]. At high temperature the diffusion of As starts by the formation of V–As pairs, which can migrate to form V–As_2 complexes [27]. The calculations predict that these complexes can diffuse until they stop at the substitutional As forming the V–As_3 complex. In perfect agreement with this theoretical scheme, the stable V–As_3 complex is observed in the experiments in the Si([As] = 10^{20} cm^{-3}) sample. Furthermore, no V–As_3 complexes are found at the lower doping level of [As] = 10^{19} cm^{-3}, most likely because the average distance

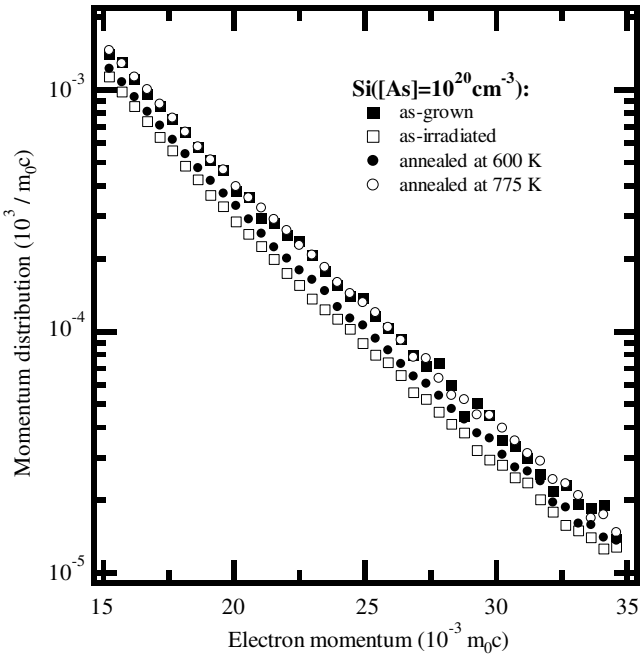

Figure 6. The high-momentum part of the positron–electron momentum distribution at the various vacancy–impurity pairs identified in as-grown and irradiated Si([As] = 10^{20} cm^{-3}) after various annealings. The simple V–As pair, detected after irradiation, converts to V–As_2 and V–As_3 after annealings at 600 and 775 K, respectively [16].

between the donor atoms is too large and the migrating V–As and V–As_2 may dissociate before creating larger complexes. Stable interstitial agglomerates may also form a competing trap for the diffusing vacancy defects.

To verify the formation mechanism of V–As_3 complexes we perform an annealing experiment in the electron-irradiated Si([As] = 10^{20} cm^{-3}) sample (fluence 5×10^{18} cm^{-2}). As explained above, the dominant defects after irradiation are V–As pairs and their concentration is above 10^{18} cm^{-3}. The positron trapping remains in saturation over the whole annealing series up to 900 K, indicating that the vacancies survive with high concentrations ($>10^{18}$ cm^{-3}). The measured core electron momentum distributions (figure 6) show a clear increase in the intensity after annealings at 600 and 775 K. This effect is due to the increase of annihilations with the 3d electrons of As surrounding the vacancy. Comparisons with theory and experiment (figures 5 and 6) indicate that the dominant vacancy defect is V–As_2 after 600 K and V–As_3 after 775 K annealings, respectively. The results thus show that the migration of V–As pairs at 450 K (estimated activation energy 1.3(2) eV) leads to the formation of V–As_2 complexes, which in turn convert to stable V–As_3 complexes at 700 K (activation energy 2.0 eV). These observations are consistent with previous results obtained by EPR [30, 31] and deep-level transient spectroscopy [32]. The estimated activation energies are in very good agreement with the theoretical calculations of migration barriers by Xie and Chen [28].

The concentration of free electrons in heavily doped Si saturates at $\leqslant 5 \times 10^{20}$ cm^{-3} due to the formation of compensating defects [3]. The present results show that V–As_3 is the dominant vacancy defect in Cz grown Si([As] = 10^{20} cm^{-3}). The migration of V–As_2 at 700–800 K explains the electrical deactivation observed in low-temperature grown and laser-treated

samples during post-growth annealing [3, 33]. Our recent data show that $V–As_3$ is dominant also in MBE Si doped by 1 keV As implantation during growth at 450 °C, although even larger clusters such as $V_2–As_5$ also exist [17]. The $V–As_3$ and $V_2–As_5$ defects can be removed by annealings at 800 and 900 °C, respectively, which increases the electrical activity of doping. The rapid thermal annealing leads to the lowest concentrations of these deactivating defects, indicating that their formation is limited by migration processes during the cooling down [17].

5. Conclusions

The present results show that positron lifetime and core electron momentum distribution experiments can yield detailed information on the open volume and atomic surrounding of vacancy complexes in Si. In electron-irradiated material, we identify divacancies, V–O complexes and vacancies paired with single P and As dopant impurities. In as-grown Cz and MBE Si we observe the formation of vacancy defects when the As doping level increases to 10^{20} cm^{-3}. The dominant native defect is identified as a monovacancy surrounded by three As atoms. We verify experimentally the formation mechanism of $V–As_3$; the migration of V–As pairs at 450 K leads to the formation of $V–As_2$ complexes, which in turn convert to stable $V–As_3$ defects at 700 K. The formation of the $V–As_3$ complex is consistent with the theoretical predictions of the As diffusion and electrical deactivation in highly doped Si.

Acknowledgments

The authors thank Dr M Hakala and Professor M J Puska for collaboration and for providing the results of theoretical calculations. They are also grateful for Dr H Kauppinen and Dr J Nissilä for assistance in some of the experiments.

References

[1] Watkins G D 1986 *Deep Centers in Semiconductors* ed S Pantelides (New York: Gordon and Breach) p 147
[2] Packan P A 1999 *Science* **285** 2079
[3] Lietoila A, Gibbons J F and Sigmon T W 1980 *Appl. Phys. Lett.* **36** 765
[4] Fahey P M, Griffin P B and Plummer J D 1989 *Rev. Mod. Phys.* **61** 289
[5] Pandey K C, Erbil A, Cargill G S III, Boehme R F and Vanderbilt D 1988 *Phys. Rev. Lett.* **61** 1282
[6] Ramamoorthy M and Pantelides S T 1996 *Phys. Rev. Lett.* **76** 4753
[7] Chadi D J, Citrin P H, Park C H, Adler D L, Marcus M A and Gossmann H-J 1997 *Phys. Rev. Lett.* **79** 4834
[8] Lawther D W, Myler U, Simpson P J, Rousseau P M, Griffin P B and Plummer J D 1995 *Appl. Phys. Lett.* **67** 3575
[9] Myler U, Goldberg R D, Knights A P, Lawther D W and Simpson P J 1996 *Appl. Phys. Lett.* **69** 3333
[10] Szpala S, Asoka-Kumar P, Nielsen B, Peng J P, Hayakawa S, Lynn K G and Gossmann H-J 1996 *Phys. Rev.* B **54** 4722
[11] Voyles P M, Muller D A, Grazul J L, Citrin P H and Gossmann H-J L 2002 *Nature* **416** 826
[12] Saarinen K, Hautojärvi P and Corbel C 1998 *Identification of Defects in Semiconductors* ed M Stavola (New York: Academic) p 209
[13] Krause-Rehberg R and Leipner H S 1999 *Positron Annihilation in Semiconductors* (Heidelberg: Springer)
[14] Alatalo M, Kauppinen H, Saarinen K, Puska M J, Mäkinen J, Hautojärvi P and Nieminen R M 1995 *Phys. Rev.* B **51** 4176
[15] Saarinen K, Nissilä J, Kauppinen H, Hakala M, Puska M J, Hautojärvi P and Corbel C 1999 *Phys. Rev. Lett.* **82** 1883
[16] Ranki V, Nissilä J and Saarinen K 2002 *Phys. Rev. Lett.* **88** 105506
[17] Ranki V, Saarinen K, Fage-Pedersen J, Lundsgaard Hansen J and Nylandsted Larsen A 2003 *Phys. Rev.* B **67** 021210(R)
[18] Alatalo M, Barbiellini B, Hakala M, Kauppinen H, Korhonen T, Puska M J, Saarinen K, Hautojärvi P and Nieminen R M 1996 *Phys. Rev.* B **54** 2397

[19] Hakala M, Puska M J and Nieminen R M 1998 *Phys. Rev.* B **57** 7621
[20] Puska M J and Nieminen R M 1994 *Rev. Mod. Phys.* **66** 841
[21] Boronski E and Nieminen R M 1986 *Phys. Rev.* B **34** 3820
[22] Kauppinen H, Corbel C, Nissilä J, Saarinen K and Hautojärvi P 1998 *Phys. Rev.* B **57** 12911
[23] Mäkinen J, Corbel C, Hautojärvi P, Moser P and Pierre F 1989 *Phys. Rev.* B **39** 10162
[24] Mäkinen J, Hautojärvi P and Corbel C 1992 *J. Phys.: Condens. Matter* **4** 5137
[25] Avalos V and Dannefaer S 1996 *Phys. Rev.* B **54** 1724
[26] Kauppinen H, Corbel C, Skog K, Saarinen K, Laine T, Hautojärvi P, Desgardin P and Ntsoenzok E 1997 *Phys. Rev.* B **55** 9598
[27] Mathiot D and Pfister J C 1983 *Appl. Phys. Lett.* **42** 1043
[28] Xie J and Chen S P 1999 *Phys. Rev. Lett.* **83** 1795
[29] Pankratov O, Huang H, Diaz de la Rubia T and Mailhiot C 1997 *Phys. Rev.* B **56** 13172
[30] Elkin E L and Watkins G D 1968 *Phys. Rev.* **174** 881
[31] Sieverts E G and Ammerlaan C A J 1977 *Radiation Effects in Semiconductors* (*Inst. Phys. Conf. Ser. 31*) p 213
[32] Nylandsted Larsen A, Christensen C and Petersen J W 1999 *J. Appl. Phys.* **86** 4861
[33] Gossmann H-J, Unterwald F C and Luftman H S 1993 *J. Appl. Phys.* **73** 8237